, ,

A_y Measurement in pp Elastic Scattering. (systematic uncertainties)

G. Macharashvili

April-2013 beam-time, Exp. 212, October 2013

1 introduction

We use the notations of Ref.[1] (L and R with indices) with some minor modifications. In this notation the indeces refer to the right and left telescopes an L corresponds to the placement of telescope with respect to the beam polarization direction. The alternative notations are taken from Ref.[2] (L and R with up and down arrows). In this case L and R correspond to the telescopes placement with respect to y axis (directed upwards) in lab system and the arrow shows the beam polarization direction. Number of events detected at the up-polarized beam:

$$N_1(\vartheta,0) \equiv L_1 = L\uparrow = B_\uparrow \cdot \Omega_1 \ (1 + P_\uparrow \langle cos\phi\rangle_1 A(\vartheta)) \tag{1}$$

$$N_2(\vartheta,\pi) \equiv R_2 = R\uparrow = B_\uparrow \cdot \Omega_2 \ (1 - P_\uparrow \langle cos\phi\rangle_2 A(\vartheta)) \tag{2}$$

Number of events detected at the down-polarized beam:

$$N_1(\vartheta,\pi) \equiv R_1 = L\downarrow = B_\downarrow \cdot \Omega_1 \ (1 - P_\downarrow \langle cos\phi\rangle_1 A(\vartheta)) \tag{3}$$

$$N_2(\vartheta,0) \equiv L_2 = R\downarrow = B_\downarrow \cdot \Omega_2 \ (1 + P_\downarrow \langle cos\phi\rangle_2 A(\vartheta)) \tag{4}$$

where $P_{\uparrow\downarrow}\langle cos\phi\rangle_i$ are the beam polarization *effective* values for up and down polarizations for the $i-th$ detector, $B_{\uparrow\downarrow}$ are the luminocities of up and down polarized beams respectively, Ω_i is the efficiency of $i-th$ detector integrated on the solid angle. ϑ always denotes the scattering angle in the c.m. system. The scattering angle used for the analysis is defined by the kinetic energy of the detected (recoil) particle. The geometrical recoil angle is measured with larger uncertainties. From now on we use P to denote the *effective* beam polarization omitting the $\langle cos\phi\rangle$ factor.

If we form the geometric means

$$L = \sqrt{L_1 L_2} = \sqrt{L\uparrow R\downarrow} \tag{5}$$

$$R = \sqrt{R_1 R_2} = \sqrt{L{\downarrow}R{\uparrow}} \tag{6}$$

In case the detectors efficiencies do not change during the run and $P_\uparrow = P_\downarrow$, $A_1 = A_2$, and the average $\langle cos\phi \rangle$'s are equal, the following formulae were used to estimate the asymmetry and its statistical uncertainty in each ϑ interval.

$$\varepsilon = \frac{L - R}{L + R} = PA \tag{7}$$

$$\sigma_\varepsilon = \frac{L\,R}{(L+R)^2}\sqrt{\frac{1}{L_1} + \frac{1}{L_2} + \frac{1}{R_1} + \frac{1}{R_2}} \tag{8}$$

So the analyzing power is defined as

$$A = \frac{\varepsilon}{P} \quad \text{with the uncertainty} \quad \sigma_A = A\sqrt{\left(\frac{\sigma_\varepsilon}{\varepsilon}\right)^2 + \left(\frac{\sigma_P}{P}\right)^2}. \tag{9}$$

Some additional information can be extracted from the following asymmetries (the formulae are taken from [2]):

$$\begin{aligned}\alpha_{10}[2] &= \frac{\sqrt{L_\uparrow L_\downarrow} - \sqrt{R_\uparrow R_\downarrow}}{\sqrt{L_\uparrow L_\downarrow} + \sqrt{R_\uparrow R_\downarrow}} = \frac{\sqrt{L_1 R_1} - \sqrt{L_2 R_2}}{\sqrt{L_1 R_1} + \sqrt{L_2 R_2}} \\ &= \varepsilon_\Omega + \frac{PA}{1 - P^2A^2}\varepsilon_P - \frac{P^2A^2}{1 - P^2A^2}\varepsilon_A + \mathcal{O}(\varepsilon^3)\,;\end{aligned} \tag{10}$$

$$\begin{aligned}\alpha_{11}[2] &= \frac{\sqrt{L_\uparrow R_\uparrow} - \sqrt{L_\downarrow R_\downarrow}}{\sqrt{L_\uparrow R_\uparrow} + \sqrt{L_\downarrow R_\downarrow}} = \frac{\sqrt{L_1 R_2} - \sqrt{L_2 R_1}}{\sqrt{L_1 R_2} + \sqrt{L_2 R_1}} \\ &= \varepsilon_B + \frac{PA}{1 - P^2A^2}\varepsilon_A - \frac{P^2A^2}{1 - P^2A^2}\varepsilon_P + \mathcal{O}(\varepsilon^3)\,;\end{aligned} \tag{11}$$

In these two asymmetries the parameters ε_Ω and ε_B dominate. They are not supposed to be small but they cancel in eq.(15) (see below). So we can not extract ε_P. The asymmetry ε_B could be defined independently asumming `Trig_out` counter is proportional to the luminosity.

It has to be stressed that the luminosity (B) and the dead-time differences for up and down polarized beams do not cause the systematics.

Below we consider all (hopefully almost all) possible systematics sources and estimate the systematic errors and systematic uncertainties. Numerical tests were performed to estimate for some sources of systematics listed below.

2 sources of the systematic uncertainties

Let's define the beam up and down polarization modules in the following way:

$$P_{\uparrow\downarrow} = P(1 \pm \varepsilon_P)\,, \quad \text{with} \quad P = 0.5\,(P_\uparrow + P_\downarrow)\,, \quad \text{and} \quad \varepsilon_P = \frac{P_\uparrow - P_\downarrow}{P_\uparrow + P_\downarrow}\,, \tag{12}$$

In case of single-sided detector the beam polarization up/down modules inequality influences the measured asymmetry at a first order, and changes it as follows

$$\varepsilon \,=\, PA \quad \rightarrow \quad \varepsilon = \frac{PA}{1 + \varepsilon_P PA}\,, \tag{13}$$

and respectively

$$A \,=\, \frac{\varepsilon}{P} \cdot \frac{1}{1 - \varepsilon\varepsilon_P}\,. \tag{14}$$

In case of double-sided detector with stable detector efficiences, the beam polarization up/down inequality ($\varepsilon_P \neq 0$), and the detectors misalignment ($\varepsilon_A \neq 0$) affect the measured asymmetry at the second order:

$$\begin{aligned}\alpha_9[2] \,\equiv\, \varepsilon \,&=\, \frac{\sqrt{L_\uparrow R_\downarrow} - \sqrt{R_\uparrow L_\downarrow}}{\sqrt{L_\uparrow R_\downarrow} + \sqrt{R_\uparrow L_\downarrow}} \,=\, \frac{\sqrt{L_1 L_2} - \sqrt{R_1 R_2}}{\sqrt{L_1 L_2} + \sqrt{R_1 R_2}} \\ &= PA\left[1 - \frac{2\,PA}{1 - P^2A^2}\,\varepsilon_P\varepsilon_A + \frac{P^2A^2}{1 - P^2A^2}\,(\varepsilon_P^2 + \varepsilon_A^2)\right] + \mathcal{O}(\varepsilon^4)\,;\end{aligned} \tag{15}$$

This equation is the exact version of eq.(7) up to 4-th order in small quantity.

2.1 ε_A, the detectors misalignment effect

The asymmetry of analyzing power ε_A in eq.(15) comes from misalignment of the left and right detectors, so the measured angles ϑ_1 and ϑ_2 are different. Corresponding asymmetry is defined in the following way

$$\varepsilon_A \,=\, \frac{A(\vartheta_1) - A(\vartheta_2)}{A(\vartheta_1) + A(\vartheta_2)}, \tag{16}$$

$$\text{with} \quad A(\vartheta) \,=\, 0.5\,(A(\vartheta_1) + A(\vartheta_2)) \quad \text{and} \quad A(\vartheta_1) - A(\vartheta_2) \,=\, \frac{\partial A}{\partial \vartheta}\,(\vartheta_1 - \vartheta_2)\,, \tag{17}$$

where $\vartheta = 0.5\,(\vartheta_1 + \vartheta_2)$. We calculated ε_A numerically assuming[1] $|\vartheta_1 - \vartheta_2| \simeq (0.5 \pm 1.0)^o$ for each ϑ bin. To estimate $\frac{\partial A}{\partial \vartheta}$ we fitted the measured $A(\vartheta)$ with parabola ($\chi^2/ndf = 16.6/19$). The calculated ε_A does not exceed 0.03 in the whole angular range (see Fig.1). Maximum value of the factor $2PA/(1 - P^2A^2)$ calculated using the measured A and P, equals to 0.5 at the beam energy of $0.8\,GeV$. Assuming $\varepsilon_P = 0.10$ (the most unfavorable case), the upper limit of the $\varepsilon_P\varepsilon_A$ term in eq.(15) equals to 0.0015. At the higher energies the factor is about 2 times lower.

So the systematic error (fake asymmetry) induced by the detectors misalignment can be ignored in the second and the fourth terms of eq.(15).

[1] estimated from $\vartheta - \vartheta(E)$ distribution variance.

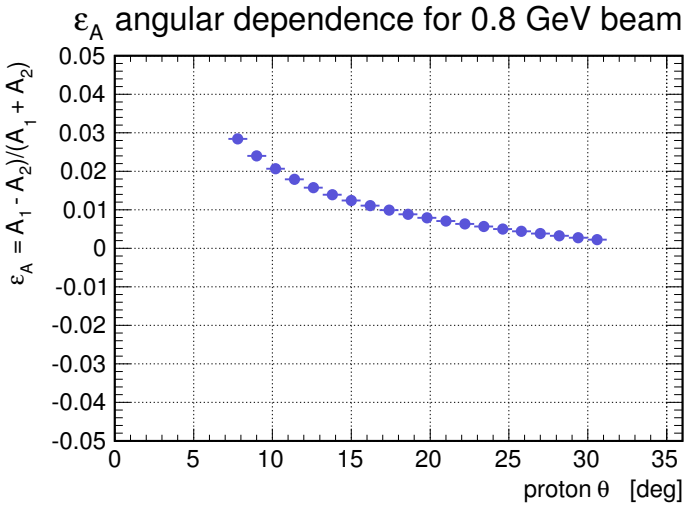

Fig. 1: ε_A estimate for the left and right telescopes ϑ measurement difference of 0.5^o.

2.2 ε_P, beam up and down polarization inequality

We estimated the upper limit of the factor $P^2A^2/(1-P^2A^2)$ in eq.(15) for all beam energies. The factor does not exceed 0.05 (the worst case at $0.8\,GeV$ beam and $\vartheta = 30^o$). At the higher energies the factor is about 2 times lower due to low A. For higher beam energies the factor is less than 0.02. The simulated angular dependence of the factor is shown in Fig.2. Assuming $\varepsilon_P = 0.10$ (this means that at $P = 0.5$ the absolute difference $P_\uparrow - P_\downarrow = 0.10$) the correction term is less than $0.0005\,A$. More precisely the systematic error in $A(\vartheta)$ induced by ε_P (its angular dependence) is shown in Fig.2.

So we ignore the polarization up and down inequality influence on the measured asymmetry.

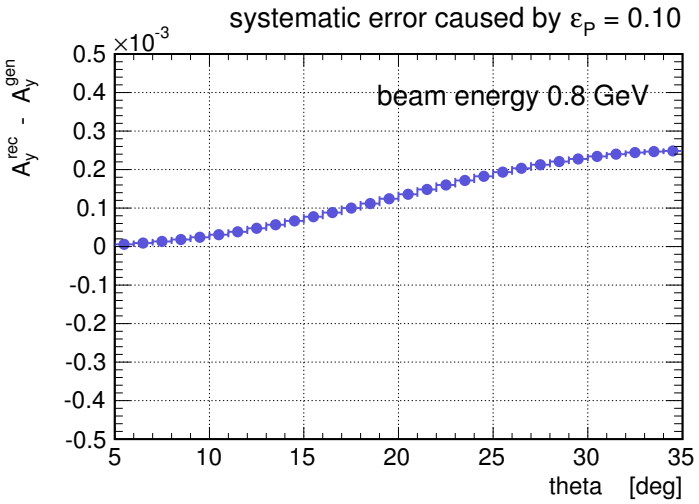

Fig. 2: The systematic error in $A(\vartheta)$ measurement at the beam energy of $0.8\,GeV$ induced by $\varepsilon_P = 0.10$ is shown. The dependence is evaluated by the simulation. The angular dependence comes from the analysing power angular dependence.

2.3 effective $\Delta\phi$ acceptance inequality

$\Delta\phi$ acceptances for the left and right detectors slightly differ in average. $\langle cos\phi\rangle_1 = 0.9663 \pm 0.0005$ and $\langle cos\phi\rangle_2 = 0.9670 \pm 0.0003$. So we assume that ϕ acceptances of the detectors are the same. The simulation shows that even at a larger difference between $\langle cos\phi\rangle_1$ and $\langle cos\phi\rangle_2$ it does not affect the measured asymmetry.

2.4 ε_Ω and the detectors efficiencies asymmetry

Let's define the left and right detectors efficiencies asymmetry:

$$\Omega_{1,2} = \Omega(1 \pm \varepsilon_\Omega)\,, \quad \text{with} \quad \Omega = 0.5\,(\Omega_1 + \Omega_2)\,, \quad \text{and} \quad \varepsilon_\Omega = \frac{\Omega_1 - \Omega_2}{\Omega_1 + \Omega_2}\,, \tag{18}$$

The asymmetry ε_Ω in general is not necessarily small. The efficiency asymmetry can be estimated using eq.(10). The angular dependence of the asymmetry ε_Ω is shown in Fig.3.

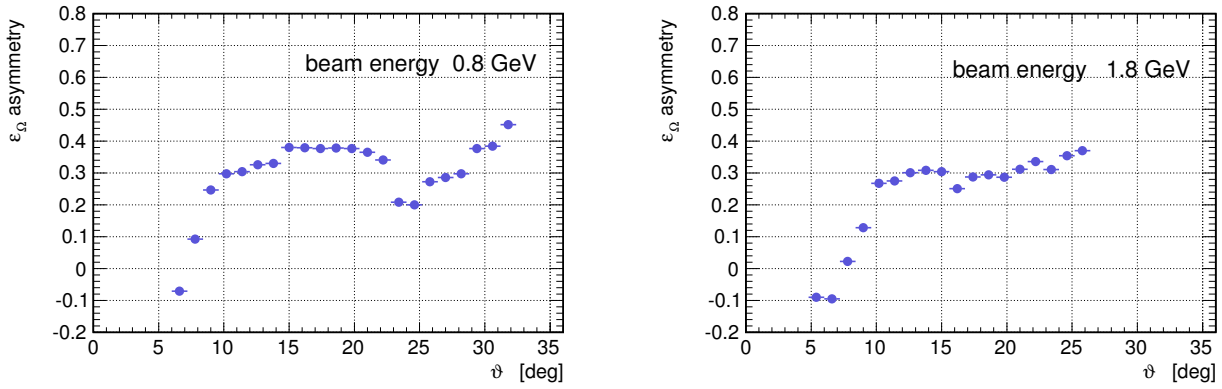

Fig. 3: ε_Ω angular dependences at the beam energies of 0.8 (*left panel*) and $1.8\,GeV$ (*rightt panel*). $\varepsilon \simeq 0.3$ means that the positive side telescope and its triggering unit are about 2 times more effective.

2.5 the detectors efficiencies stability

Eq.(15) shows that ε_Ω does not affect the measured asymmetry. But the problem is the efficiencies stability in time. The only factor that could affect the asymmetry measured with such a two-arm detector is any instability in the reatio of the efficiencies of the left and right telescopes.

Let's introduce the efficiencies ratios for beam up and down polarizations

$$\omega_\uparrow = \frac{L_1}{R_2} \equiv \frac{L_\uparrow}{R_\uparrow} = r_\uparrow \frac{1 + P_\uparrow A}{1 - P_\uparrow A} \quad \text{with} \quad r_\uparrow = \left(\frac{\Omega_1}{\Omega_2}\right)_\uparrow\,, \tag{19}$$

$$\omega_\downarrow = \frac{R_1}{L_2} \equiv \frac{L_\downarrow}{R_\downarrow} = r_\downarrow \frac{1 - P_\downarrow A}{1 + P_\downarrow A} \quad \text{with} \quad r_\downarrow = \left(\frac{\Omega_1}{\Omega_2}\right)_\downarrow , \tag{20}$$

It is impossible to evaluate $r_\uparrow$ and $r_\downarrow$ directly but we can measure $w_\uparrow$ and $w_\downarrow$. Now we can introduce the asymmetry which we can estimate for each ϑ bin:

$$\varepsilon_\omega = \frac{\omega_\uparrow - \omega_\downarrow}{\omega_\uparrow + \omega_\downarrow}, \quad \text{in case} \quad r_\uparrow = r_\downarrow \;\rightarrow\; \quad \varepsilon_\omega = \frac{2\,PA}{1 + P^2A^2(1 - \varepsilon_P^2)} \simeq \frac{2\,PA}{1 + P^2A^2}, \tag{21}$$

and the ratio

$$\frac{\omega_\uparrow}{\omega_\downarrow} = \frac{r_\uparrow}{r_\downarrow} \frac{1 + 2PA + P^2A^2(1 - \varepsilon_P^2)}{1 - 2PA + P^2A^2(1 - \varepsilon_P^2)} \simeq \frac{r_\uparrow}{r_\downarrow} \frac{1 + 2PA + P^2A^2}{1 - 2PA + P^2A^2} = \frac{r_\uparrow}{r_\downarrow} \frac{(1 + PA)^2}{(1 - PA)^2}. \tag{22}$$

The *instability factor* $r_\uparrow/r_\downarrow$ equals to 1 in case the detectors average efficiencies ratio $\left(\frac{\Omega_1}{\Omega_2}\right)^2$ is the same for the beam up and down polarizations. As A_y is positive in the whole angular range at all energies the factor $(1 - PA)^2(1 + PA)^{-2} < 1$.

Keeping the average ratios constant during the simultaneously analyzed runs guarantees that it does not induce the fake asymmetry (in other words the systematic error) even the individual efficiencies change. The angular dependence of typical average ratio $r_\uparrow/r_\downarrow$ at the beam energies of 0.8 and $1.8\,GeV$ are shown in Fig.4. The fit values for all beam energies are shown in Table 5. In almost all cases the fitted constants are close to 1 (with $\chi^2/ndf \leq 1$). This means that the detector instability does not induce the fake asymmetry (see eq.(25)). Even more, it indicates indirectly that one can ignore the beam polarization asymmetry ε_P. The uncertainty of the fitted constant can be interpreted as the systematic uncertainty induced by the detector instability. Altough this uncertainty is much less than that coming from the beam polarization measurement.

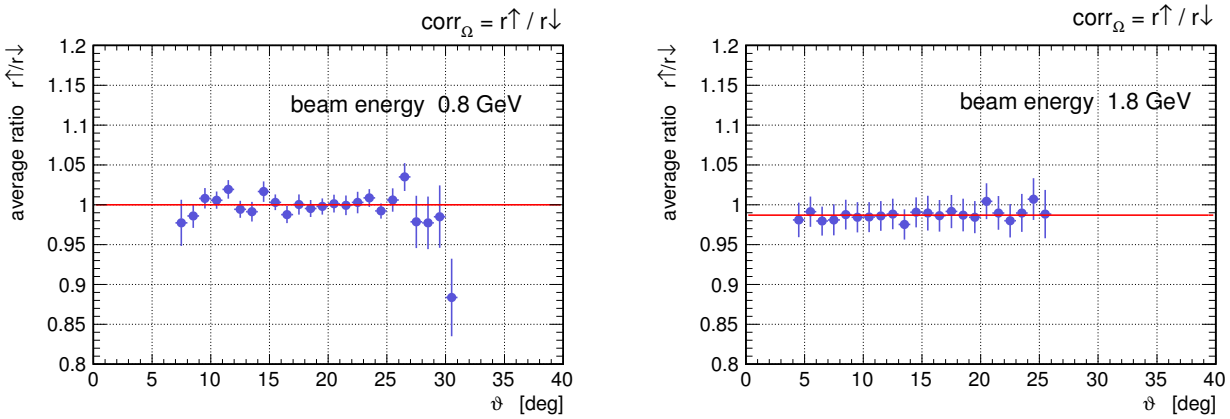

Fig. 4: The correction factor $c_\Omega = 1 - r_\uparrow/r_\downarrow$ angular dependences at the beam energies of 0.8 (*left panel*) and $1.8\,GeV$ (*rightt panel*). The fitted value of the correction factor equals to 0.0132 ± 0.0043 at the beam energy of $1.8\,GeV$.

[2]It is not necessary to require the stability of Ω_1 and Ω_2 individually (see eq.(7)).

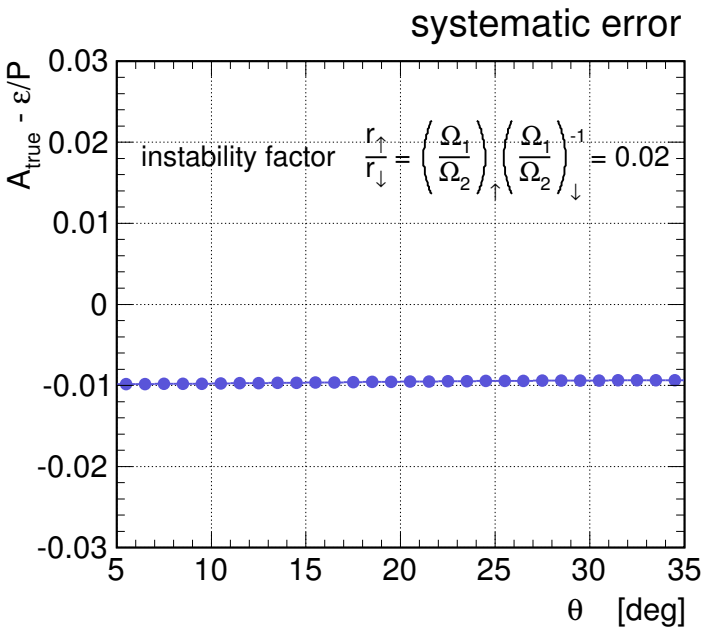

Fig. 5: The systematic error (fake asymmetry) angular dependence at the beam energy of $0.8\,GeV$ and the instability factor $r_\uparrow/r_\downarrow = 0.02$. The dependence is evaluated by simulation. NB: systematic uncertainty is taken equal to zero altough it can be estimated by the measured instability factor variance. (see Fig.4).

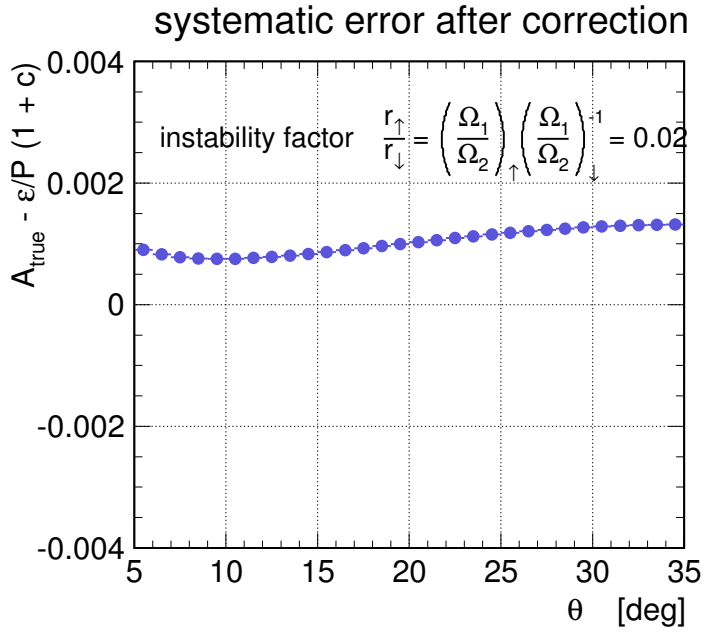

Fig. 6: The systematic error (fake asymmetry) angular dependence with the instability factor $r_\uparrow/r_\downarrow = 0.02$ (see Fig.5) after correction. The dependence is evaluated by simulation.

We performed the simulation calculation to estimate ε_w influence on the measured A. We defined the instability correction factors $\frac{r_\uparrow}{r_\downarrow}$ for each ϑ bin independently (see Fig.4). The simulation showed that the systematic error in the measured A depends on the efficiency instability factor in first order

$$\Delta A(\vartheta) \simeq \left(1 - \frac{r_\uparrow}{r_\downarrow}\right) A(\vartheta) \equiv c_\Omega(\vartheta)\, A(\vartheta)\,. \tag{23}$$

The exact dependence of the analyzing power correction factor c_Ω on the detector efficiencies ratio instability can be deduced from eq.(7):

$$c_\Omega = \frac{1 + P^2A^2}{2PA}\left(1 - \sqrt{\frac{r_\uparrow}{r_\downarrow}}\right). \tag{24}$$

So we corrected the measured $A(\vartheta)$ in the following way

$$A(\vartheta) \rightarrow A(\vartheta)\,(1 + c_\Omega(\vartheta))\,. \tag{25}$$

In Fig.5 the typical simulated angular dependence of the systematic error on the instability factor is shown at the beam energy of $0.8\,GeV$. The same angular dependence after correctios applied is shown in Fig.6. After correction the absolute value of the systematic error decreases in average about 10 times.

The averaged values of the correction factors c_Ω estimated using the obtained experimental data for each beam energy are shown in Table.5.

2.6 ε_B, luminosities asymmetry

Inequality of integrated luminosities for up and down polarizad beams can be described also in terms of asymmetry:

$$B_{\uparrow\downarrow} = B(1 \pm \varepsilon_B)\,, \quad \text{with} \quad B = 0.5\,(B_\uparrow + B_\downarrow)\,, \quad \text{and} \quad \varepsilon_B = \frac{B_\uparrow - B_\downarrow}{B_\uparrow + B_\downarrow}\,, \tag{26}$$

Again, ε_B is not supposed to be zero but it cancels in the asymmetry calculation eq.(15). The luminosity asymmetry can be estimated using eq.(11).

2.7 beam polarization measurement with the EDDA detector

The beam polarization was measured by the EDDA detector [3] at the end of each cycle. The cycle duration equals $180\,sec$ so we ignored the beam depolarization during the cycle. The average beam polarization was calculated averaging the beam polarization with weigths cycle by cycle. We calculated the weighted average using as a weight of each cycle the number of selected events. EDDA can not measure the beam polarization for individual cycle, but only for the pair of cycles. We calculated the beam polarization using the current cycle and the previous one with the opposite

direction of the beam polarization. In case of a missing cycle data (due to manual restart of the EDDA DAQ some runs were missed) the averaged value of the beam polarization was applied for the cycle. We used the averaged over all analyzed cycles value of the beam polarization with high statistical significance. So the statistical uncertainty can be ignored (see Table 5).

The beam polarization in each cycle is different with nearly gauss distribution. We estimated the ditribution rms for each beam energy. The distributions of the beam polarization in cycles are shown in Figs.15-20 in Appendix A. These distributions demonstrate the performance of the COSY polarized beam source and the beam polarization stability during acceleration.[3] The relative uncertainties of the beam polarization in a cycle are shown in Table.5. *These uncertainties can't be associated with the EDDA measurement uncertainty.*

reference	$\langle \Delta A_y \rangle$ (fitted)	χ^2/ndf	comment
[5]	-0.008 ± 0.001	12.5/17	overal $\sigma_{syst} = (+1, -0.5)\,\%$
[6]	0.005 ± 0.002	18.4/23	
[7]	-0.010 ± 0.001	11.5/3	overal $\sigma_{syst} = (+1, -0.5)\,\%$

Table 1:

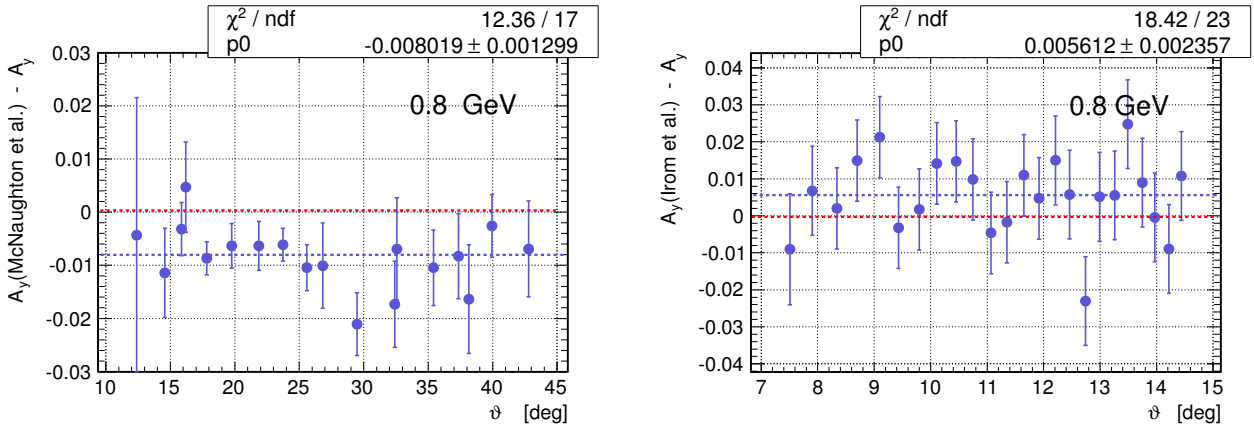

Fig. 7: The difference of the measured A with the results of two expriments [5] and [6] at the beam energy of 0.8.

2.8 beam polarization stability

In order to estimate the beam polarization stability we plotted the measured with STT asymmetry cycle by cycle (Fig.8-10) for each energy. To reduce the ststistical uncertainty we integrated the asymmetry in a large angular interval $(\Delta\vartheta)$ in the following way

[3] during acceleration the beam passes several spin resonanses

$$\varepsilon(\Delta\vartheta) \;=\; \int_{\Delta\vartheta} \varepsilon(\vartheta) d\vartheta \;=\; P \int_{\Delta\vartheta} A(\vartheta) d\vartheta \;=\; P \langle A \rangle \tag{27}$$

$\Delta\vartheta$ interval is defined as $\in [15^o, \vartheta_{max}(T_p)]$ corresponding to a larger A values. Statistical uncertainty of the measured $\varepsilon(\Delta\vartheta)$ in a cycle equals in average to 0.0035. Asumming the averaged analyzing power $\langle A \rangle$ is constant and ignoring the systematical uncertainties in $\varepsilon(\Delta\vartheta)$ measurement the variation of asymmetry depends on the statistical uncertainties of the measurement and on the polarization variations. The following formulamake spossible to estimate the later:

$$\left(\frac{\sigma\varepsilon_{tot}}{\varepsilon}\right)^2 \;=\; \left(\frac{\sigma\varepsilon_{stat}}{\varepsilon}\right)^2 + \left(\frac{\sigma p}{p}\right)^2 . \tag{28}$$

The measured values are given in Table 2.

$T_p\,[GeV]$	$\varepsilon(\Delta\vartheta)$	$\sigma\varepsilon_{tot}$	$\sigma\varepsilon_{stat}$	σ_p	EDDA σp
0.8	0.2006	0.0094	0.0039	0.0242	0.034
1.6	0.1254	0.0096	0.0043	0.0355	0.027
1.8	0.1169	0.0120	0.0032	0.0521	0.065
2.0	0.1138	0.0101	0.0033	0.0378	0.065
2.2	0.1076	0.0121	0.0035	0.0547	0.076
2.4	0.0794	0.0080	0.0034	0.0404	0.049

Table 2: In the last column we give the beam polarization variation cycle by cycle as it is estimeted with EDDA measurement. The rms are taken from Fig**??**

This method of the polarization variation estimate is more accurate than the EDDA measurement but evidently it does not measure the polarization module. We conclude that the beam polariation variation (rms) equals in average to 0.04.

2.9 comparison with other experiments

The beam polarization measurement by EDDA detector was performed with $relative$ systematic uncertainties of 3% [3]. This uncertainty dominates in our final result. The close coincidence of our measurements with the results of other experiments at $0.8\,GeV$ indicates that actually the systematic errors due to P measurement are negligible. Comparison of our data with other experiments are shown in Table 1 and Fig.7.

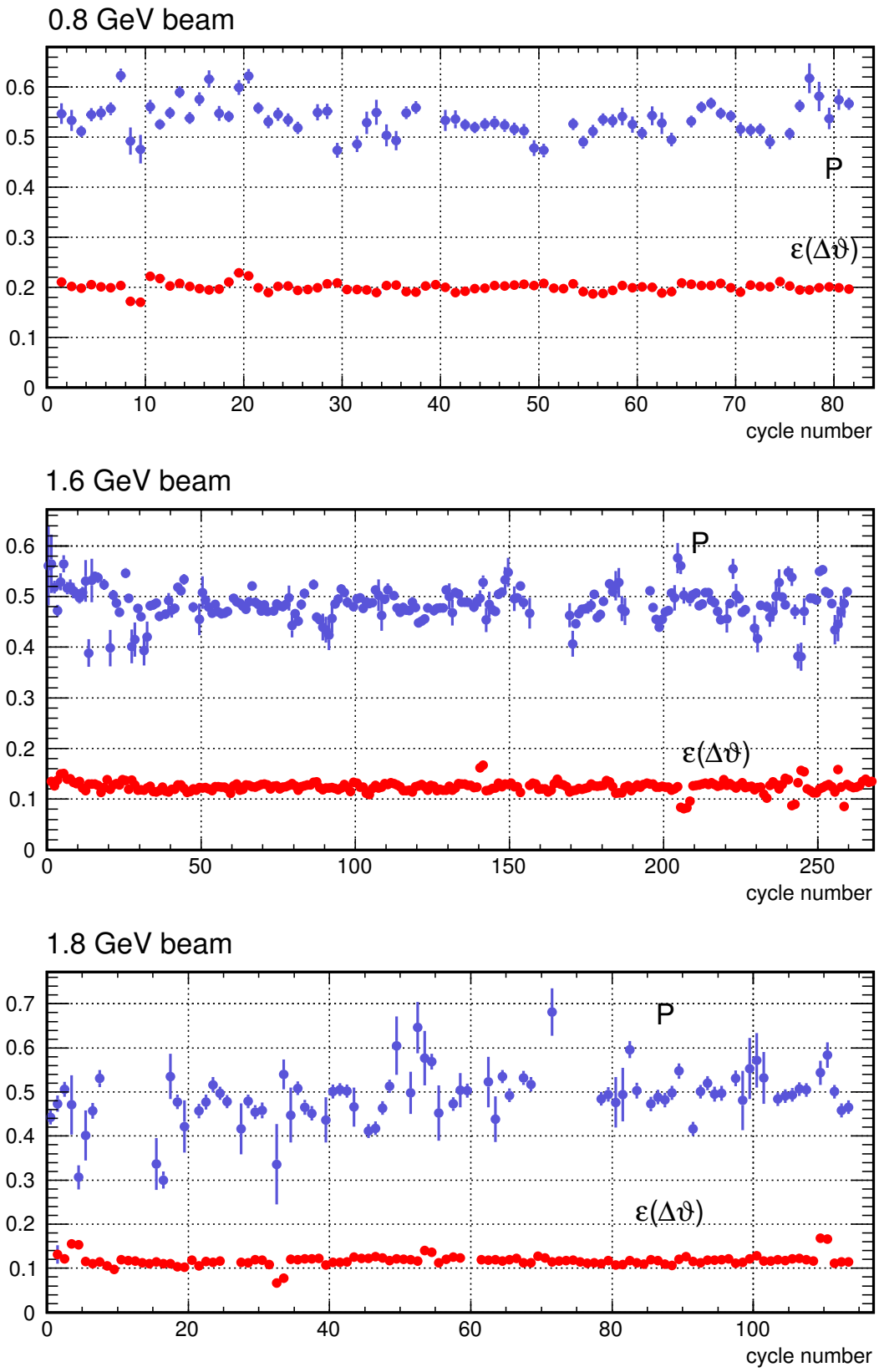

Fig. 8: Beam polarization measured with EDDA (*in blue*) and the integrated asymmetry measured with STT (*in red*) in each cycle for the beam energies of 0.8, 1.6, and 1.8 GeV.

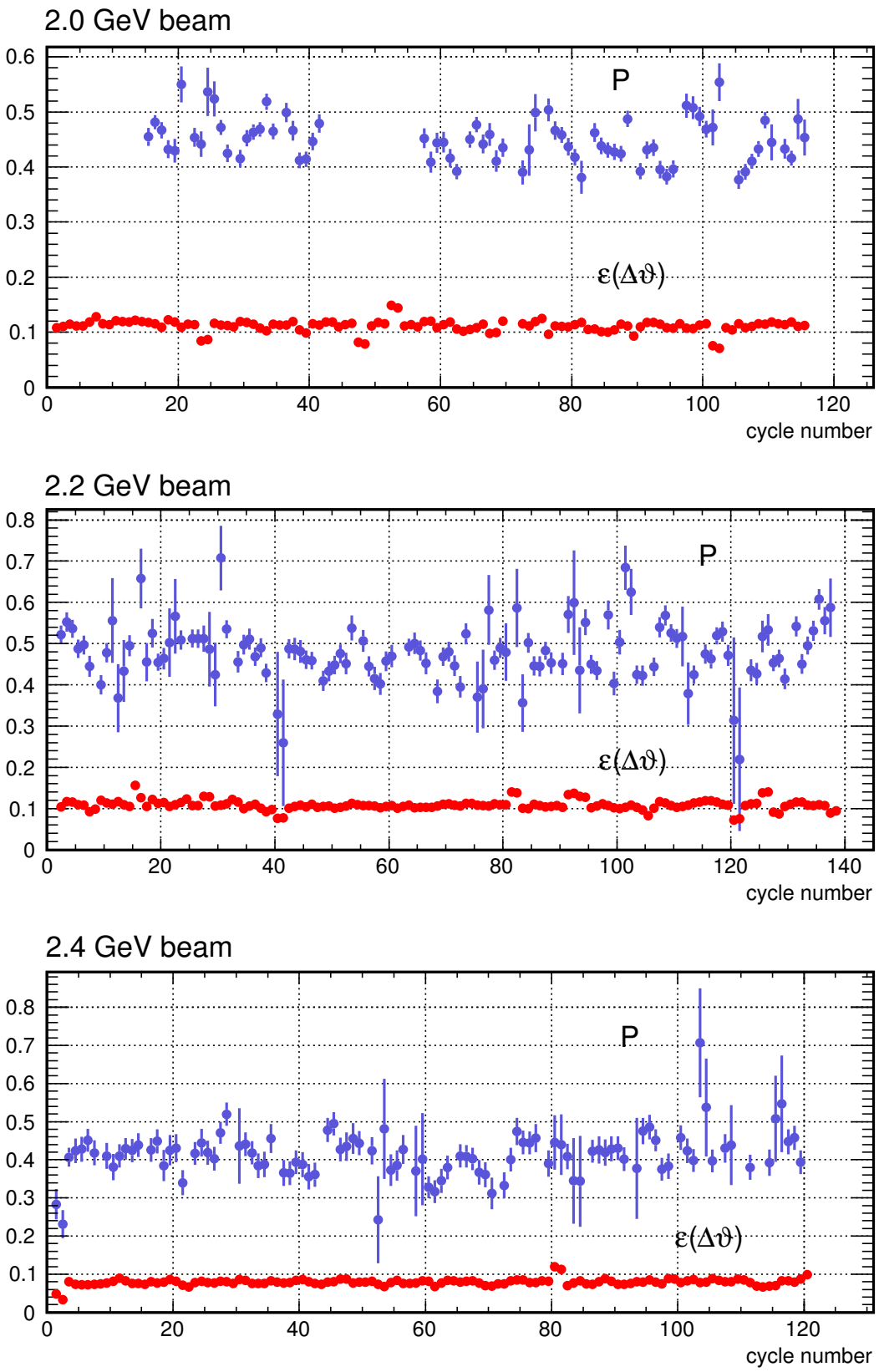

Fig. 9: Beam polarization measured with EDDA (*in blue*) and the integrated asymmetry measured with STT (*in red*) in each cycle for the beam energies of 2.0, 2.2, and 2.4 GeV.

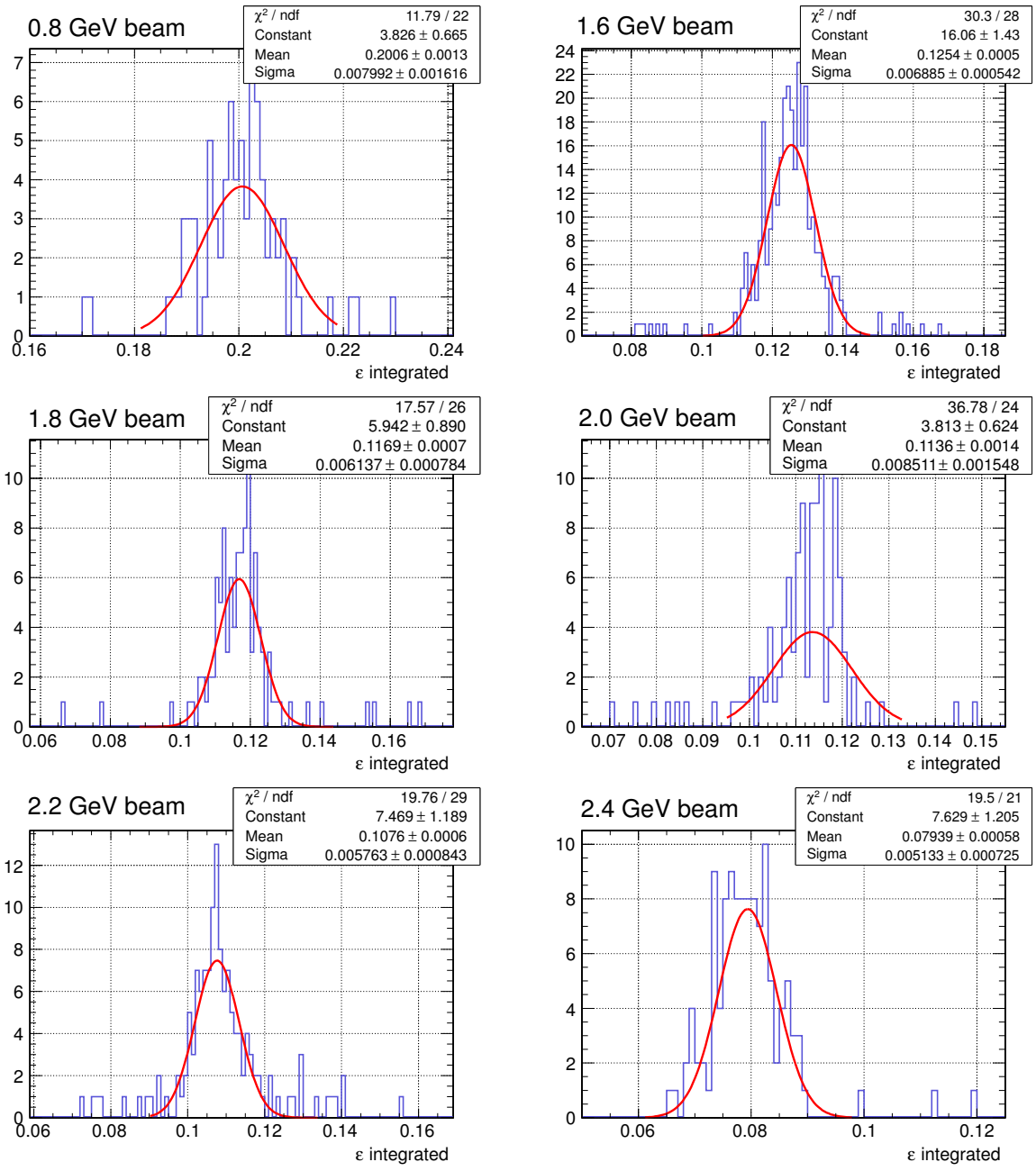

Fig. 10: The integrated asymmetry distributions for the beam energies $0.8 - 2.4\,GeV$. We asumme that the asymmetry variation comes from the beam polarization variation. The beam polarization variation (uncertainty) in average equals to 0.03.

3 analysis details

3.1 event selection

We selected the useful events applying the cuts on m_x and the vertex position. Varying the selection criteria in a reasonable ranges does not change the final results beyond $67\,\%$ of the confidence intervals $(\pm\sigma)$.

3.2 track reconstruction

The data analysis chain is described in Ref.[4]. Some tracking algorithms have been modified in order to increase the track reconstruction efficiency.

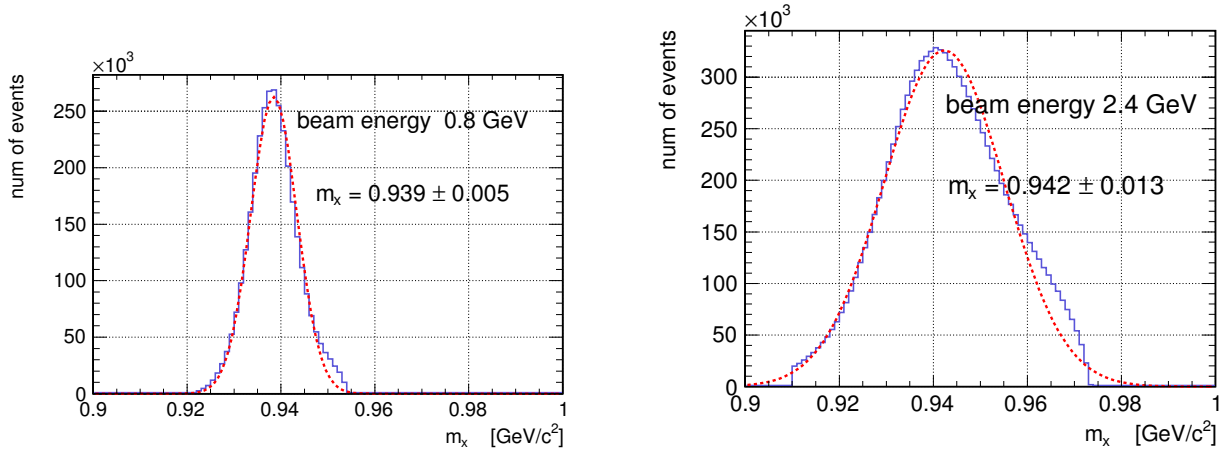

Fig. 11: Missing mass spectra for the beam energies of 0.8 and $2.4\,GeV$. The humps at the right side of the distributions come from the detector response nonlinearity.

Tracks were reconstructed in two different ways, on all three layers or on two of them when the hit is absent at the expected place in a third layer. the recostructed tracks are labeled depending on used hits (see Table 3). Typical partial density of each case depends on the telescope efficiency. The telescope efficiency itself depends on the energy range (closeness to the threshold) and the spatial inefficiency (e.g. inactive segments).

NB: in case of the track reconstruction version $0x5$ the deposited energy of $\Delta E_2 = 5\,\Delta E_1$ applied to the layer 2, and in case of the version $0x6$ the deposited energy in the layer 1 equals $\Delta E_1 = 0.2\,\Delta E_2$. This makes sure that the summary energy loss of a particle is correct.

track label	layer-1	layer-2	layer-3	% (stt-1)	% (stt-2)	
0x1	•					special case
0x3	•	•		11.2	16.6	
0x5	•		•	0.4	0.6	
0x6		•	•	57.7	53.9	
0x7	•	•	•	30.7	28.8	

Table 3: Track reconstruction versions.

label	$m_x \pm \sigma\ [MeV]$	$[\vartheta - \vartheta(E)] \pm \sigma\ [^o]$	energy range	ϑ range		
0x3	0.939 ± 0.011	0.197 ± 2.148				
0x5	0.939 ± 0.014	0.550 ± 2.518				
0x6	0.943 ± 0.017	0.323 ± 1.532				
0x7	0.938 ± 0.008	-0.005 ± 0.806				

Table 4: Track reconstruction parameters for each version. These parameters do not depend on the beam energy but only on the kinetic energy of the recoil proton.

$T_p\,[GeV]$	0.796	1.600	1.800	1.965	2.157	2.368
$\Delta t \quad [h]$	4.8	16.8	9.7	9.9	12.1	10.1
$N_{trk} \cdot 10^6$	4.1	17.2	15.2	13.9	15.4	14.3
$\vartheta_{min} - \vartheta_{max} \quad [^o]$	$6.0 - 33.0$	$3.6 - 26.4$	$3.6 - 26.4$	$3.6 - 24.0$	$3.6 - 24.0$	$3.6 - 22.8$
$\vartheta_s \quad [^o]$	22.3	15.3	15.3	14.3	13.3	13.3
P	0.554± 0.008	0.504± 0.003	0.516± 0.007	0.429± 0.008	0.501± 0.010	0.435± 0.015
$\sigma P_{cycle}/P \quad [\%]$	3.7	4.7	4.4	8.5	10.7	8.5
$\langle cos\phi \rangle$	0.967	0.966	0.966	0.966	0.966	0.967
$\langle r_\uparrow / r_\downarrow \rangle$	1.0000± 0.0028	0.9992± 0.0020	0.9876± 0.0046	0.9851± 0.0046	0.9890± 0.0040	0.9941± 0.0040
c_Ω	0.0± 0.0028	0.0008± 0.0020	0.0124± 0.0046	0.0149± 0.0046	0.0110± 0.0040	0.0059± 0.0040
$m_x \quad [MeV/c^2]$	0.939± 0.004	0.940± 0.009	0.941± 0.011	0.941± 0.012	0.940± 0.013	0.940± 0.013

Table 5: Some critical parameters for each beam energy. ϑ_s is the maximum scattering angle for stopped protons.

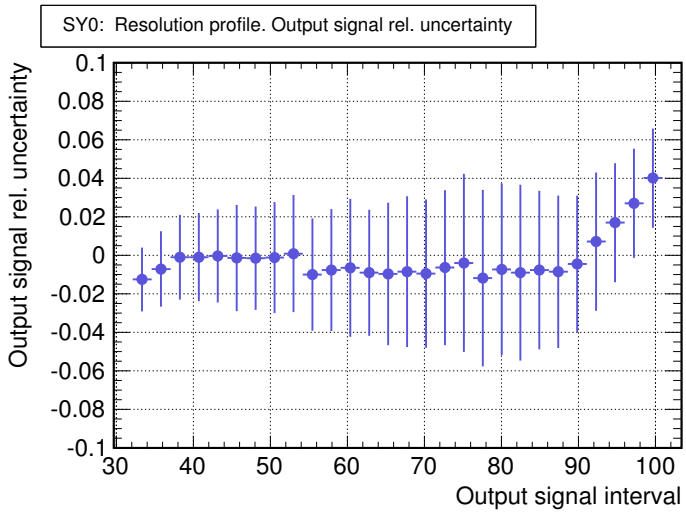

Fig. 12: The relative uncertainty of the kinetic energy reconstruction of passed protons. The uncertainty is defined by the neural network trainig procedure.

3.3 kinetic energy reconstruction for passed protons

The upper limit of the kinetic energy of stopped in the third layer protons equals to $30\,MeV$. For the protons passed the third layer the kinetic energy unambiguously can be defined by the deposited energy[4]. The kinetic energy of protons passed the third layer is reconstructed by *feed forward neural network*. The another way to define the particle kinetic energy is to resolve the equations of energy deposits in each layer with respect to the initial kinetic energy.

`Root::TMultiLayerPerceptron` class was used for neural network class generation. The *relative* uncertainty of kinetic energy reconstruction is defined during the network training procedure. It equals to 2% at $30\,MeV$ (lower limit of kinetic energy of passed protons) and to 4% at $90\,MeV$ (upper limit) (see Fig.12). Reconstruction of kinetic energies of passed protons expanded the measured kinetic energy range from 30 to $90\,MeV$ which corresponds to the acceptable scattering anglular range expansion up to $\vartheta = (22 - 33)^o$ (see Table 5) depending on the beam energy.

[4]more precisely the kinetic energy depends on ΔE_i, ϑ, and ϕ.

4 results

The results on the analysing power in $pp \to pp$ elastic scattering at 6 beam energies (0.8, 1.6, 1.8, 2.0, 2.2, and $2.4\,GeV$) are shown in Figs.13 - 14. In all these figures the SAID **??** predictions and the results of some other experiments are shown.

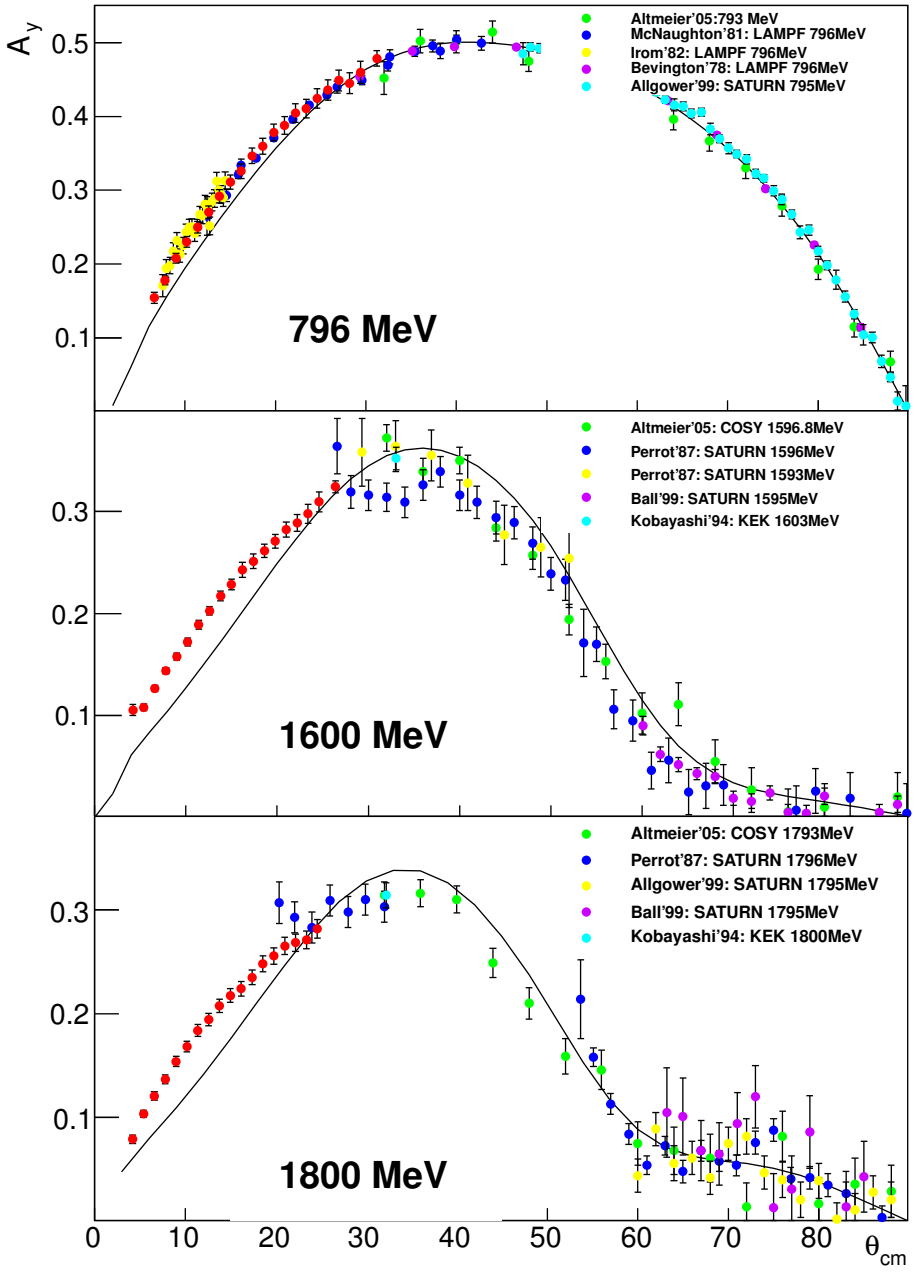

Fig. 13: Analysing powers in $pp \to pp$ elastic scattering at 0.8, 1.6, and 1.8 GeV beam energies with the SAID **??** prediction and the results of some other measurements. Statistical and instability correction uncertainties are shown.

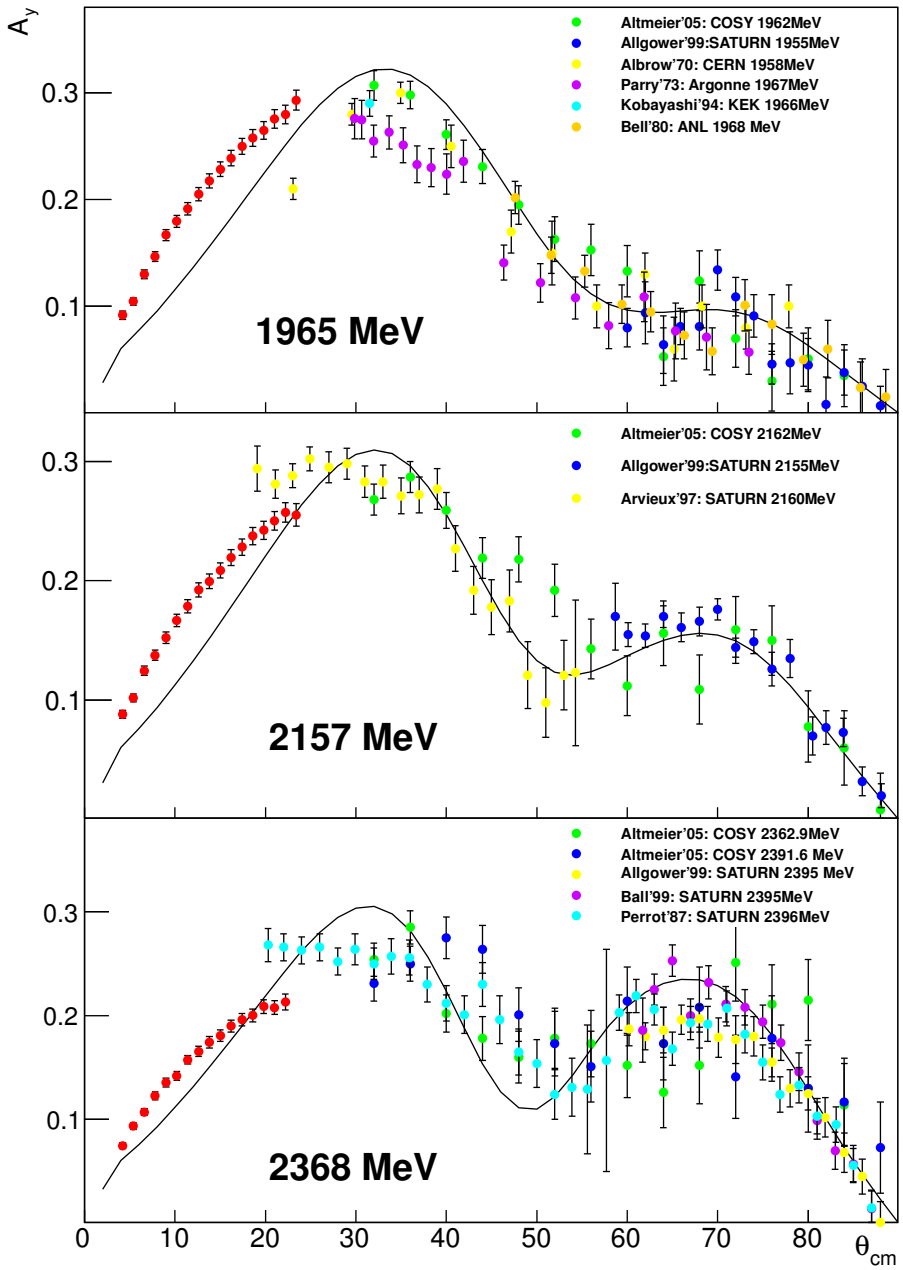

Fig. 14: Analysing powers in $pp \to pp$ elastic scattering at 2.0, 2.2, and 2.4 GeV beam energies with the SAID **??** prediction and the results of some other measurements. Statistical and instability correction uncertainties are shown.

5 conclusions

- The analysing power in $pp \to pp$ elastic scattering is measured at first time at the beam energies of $1.6 - 2.4\,GeV$ in the angular range of $4 - 26$ degree;
- The measured analysing power at the beam energy of $0.8\,GeV$ and $6^o < \vartheta < 33^o$ coincides with the results of other experiments;
- The measured analysing power at the beam energies of $\geq 1.6\,GeV$ differs from the SAID predictions (maximum difference reaches about 0.07);
- The statistical uncertainties does not exceed 0.005 in average;
- Study of the sources of the systematic errors revealed that all of them are negligible with reliable confidence. The overall relative systematic uncertainty in A_y arising from the asymmetry measurement does not exceed 0.3%;
- The detector stability control provides the systematic error correction factor compensating the left and right telescopes efficiencies ratio instability. The instability correction, which was studied at all energies, does not exceed the $|c| = 1.3\%$ that was found at $1.8\,GeV$. The relevant corrections of the analyzing power $c(\vartheta)Ay(\vartheta)$ were added for each angular bin.
- The beam polarization measurement relative uncertainty of $3\,\%$ dominates in the final results;

NB The missing mass spectra show that the background is negligible. So we didn't consider the inelastic (or some accidental) background influence on the measured asymmetry supposing that it equals to zero (see the missing mass spectra in Fig.11). Actually the asymmetry changes in the following way $\varepsilon \to \varepsilon/(1+b)$ in case of $unpolarized$ background with partial density of b. In case the background value in each ϑ bin depends on the beam polarization, the change is almost unpredictable.

References

[1] G.G. Ohlsen and P.W. Keaton, Jr. NIM, **109** (1973) 41.

[2] H. Spinka. The $50\,MeV$ Polarimeter. ANL-HEP-Pr-80-02, 1980

[3] E. Wise. Ph.D. Thesis, ISKP, Bonn, 2000

[4] http://apps.fz-juelich.de/pax/paxwiki/images/6/6c/TechNote15.pdf

[5] M.W. McNaughton *et al.* Phys.Rev.C, 23, 1128, 1981

[6] F. Irom *et al.*, Phys.Rev.C, 25, 373, 1982

[7] P.R. Bevington *et al.*, Phys.Rev.Lett, 41, 384, 1978

[8] R.A. Arndt *et al.*, Phys.Rev., C62, 034005 (2000), Phys.Rev., C76, 025209 (2007)

6 Appendix A

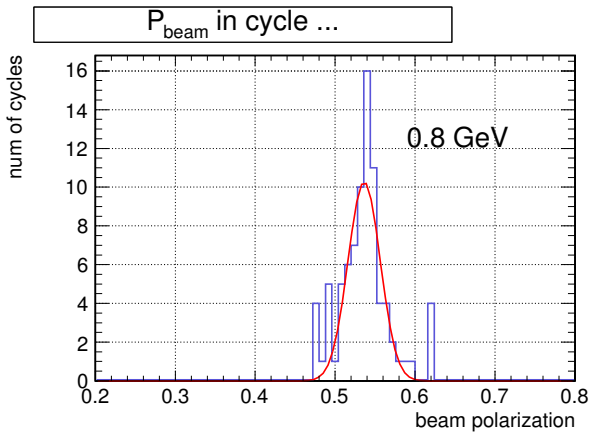

Fig. 15: The beam polarization distribution in cycles at the beam energy of $0.8\,GeV$.

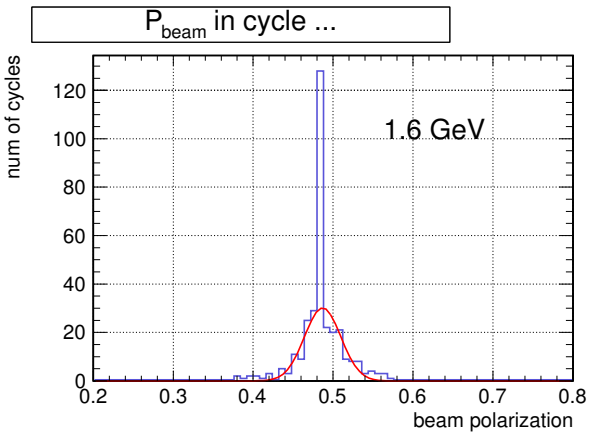

Fig. 16: The beam polarization distribution in cycles at the beam energy of $1.6\,GeV$.

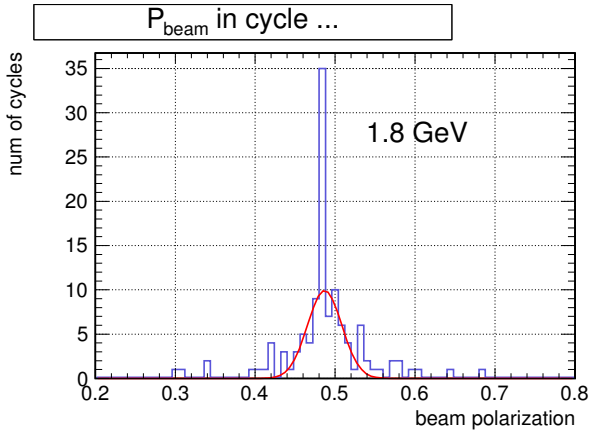

Fig. 17: The beam polarization distribution in cycles at the beam energy of $1.8\,GeV$.

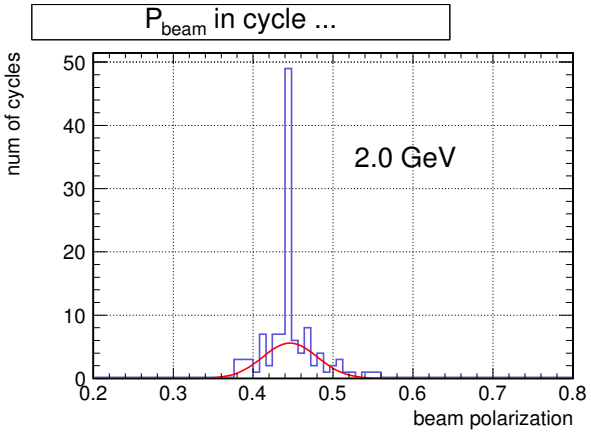

Fig. 18: The beam polarization distribution in cycles at the beam energy of $2.0\,GeV$.

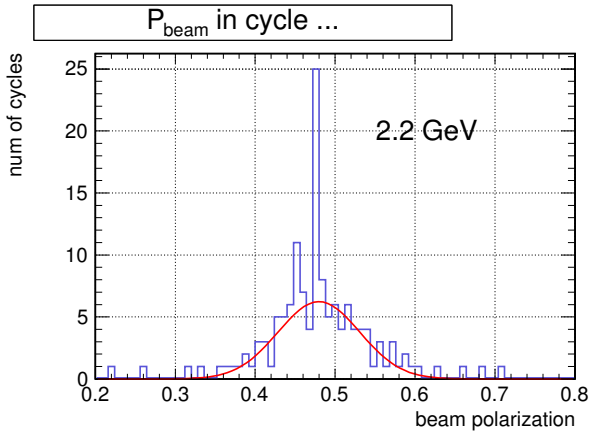

Fig. 19: The beam polarization distribution in cycles at the beam energy of $2.2\,GeV$.

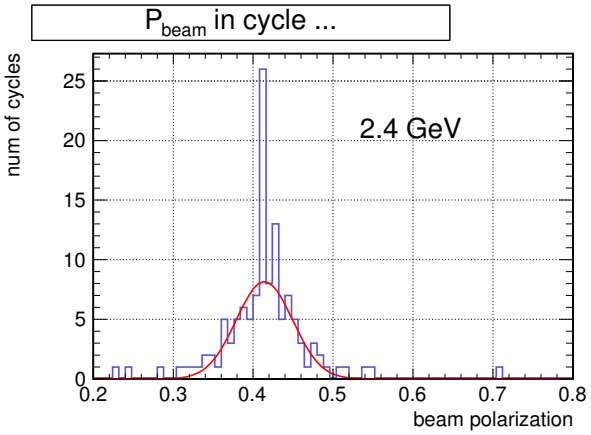

Fig. 20: The beam polarization distribution in cycles at the beam energy of $2.4\,GeV$.